



## Influence of output impedance of an inverter on its droop control strategies in a microgrid

Madhuvanthani Rajendran\*, & Sundar Govindasamy

Department of Electrical and Electronics Engineering, Sri Shakthi Institute of Engineering and Technology,  
Coimbatore 641 062, Tamil Nadu, India

*Received: 24 March 2021; Accepted: 21 September 2021*

The objective of this paper is to present a comprehensive review of the various droop control strategies employed to control the operation of the parallel inverters present in a microgrid, based on its output impedance. Predominantly, the output impedances of the inverters are inductive due to the line impedance and filter but in low power systems, the inverter has a resistive output impedance. The various categories under which the droop control strategies of inverters with inductive output impedance fall have been reviewed, along with its pros and cons. Although most of the inverters have inductive output impedance, inverters with resistive output impedance are superior due to the easier compensation of harmonics. Along with their advantages the various disadvantages present in the droop control strategies utilized for inverters with resistive output impedance and the solutions to overcome these problems are presented. Recent studies have shown that inverters with capacitive output impedance provide the lowest Total Harmonic Distortion along with reliable regulation of voltage and accurate power sharing. The technique of obtaining an inverter with capacitive output impedance along with its various advantages has also been presented. The universal droop strategy utilized for all types of inverters without prior knowledge of their output impedances is reviewed along with an example, to overcome the problem of having to change the droop equations according to the output impedance of the inverter. Lastly a few case studies related to microgrid implementation have been analyzed along with its challenges as well as standards and policies.

**Keywords:** Distributed generation, Microgrid, Inverter, Droop control technique, Output impedance

### 1 Introduction

Today, with the growing popularity of smart grids over conventional power systems, microgrids with a high percentage of sustainable energy resources may dominate the distribution system.<sup>1</sup> Distributed generation is a method that employs small-scale technologies to generate electricity close to the consumer's end.<sup>2</sup> There are two main categories that make up the Distributed Generation technologies, one being the electricity generated from renewable energy sources like wind and solar while the other being the electricity generated from alternate energy generation technologies like microturbines and fuel cells. Distributed generation can benefit the environment by reducing the amount of electricity produced by fossil fuel power plants, thereby reducing the environmental impacts of such polluting resources of electricity. Renewable energy sources like wind and solar are cost-effective technologies that are capable of being employed to generate electricity at homes as well as businesses. A conjoined heat and power system can

be utilized to channel energy that might otherwise be wasted while using distributed generation. One of the main components that form the Aggregate Technical & Commercial losses are the Transmission and Distribution losses, which can be greatly reduced or eliminated by using distributed generation which are local energy sources.

A microgrid functions like a single governable unit in connection with the grid and is defined as a group of distributed energy resources and integrated loads within distinctly outlined electrical margins. There are two distinctive working ways of a microgrid and are called the grid-connected and islanded operating modes depending on whether the microgrid is linked to the grid or disconnected from the it. There were 4,475 microgrid projects deployed during the second half of 2019 alone, which nearly represents 27GW of planned and installed capacity globally. The leader in capacity is Asia Pacific with a capacity of 9,935.4 MW, followed by North America with 8,878.6 MW and finally the combined capacities of Middle East and Africa stand at 3,627.7 MW. Nearly 70% of the global microgrid capacity is represented by remote as

\*Corresponding author (E-mail: thanira31@gmail.com)

well as industrial and commercial microgrids.<sup>3</sup> The universal microgrid market size which is valued at USD 28.6 billion in 2020 is projected to touch USD 47.4 billion by 2025.<sup>4</sup>

India, by 2030, aims on having 450 GW of renewable energy.<sup>5</sup> In order to help eliminate energy poverty and provide power to millions across India, Tata Power Renewable Microgrid foresees the development of 10,000 microgrids by 2026.<sup>6</sup> A stand-alone microgrid is a good solution to provide electricity to remote locations that are far away from the main grid. Microgrids are not only being used in remote locations in India but are also increasingly being used for commercial purposes as well as in industrial parks.<sup>7</sup> A plan to install 1000 microgrids by 2021, with a collective capacity of 500 MW was launched by the ministry of New and Renewable Energy (MNRE) in India in the year 2016. More than 500 solar microgrids (more than any other Indian state) has been installed and operated by the Chhattisgarh Renewable Energy Development Agency (CREDA). Over 75 microgrids connecting 15,000 homes and businesses has built in India and Africa by Husk Power; over the next several years the company plans an additional 300 microgrids.<sup>8</sup>

One of the most widely used power management strategies for handling the power flows between the converters present in a microgrid in a decentralized manner is the droop control method. The major benefit of the droop strategy is the nonexistence of the crucial high bandwidth communication link thereby enabling the system to be more reliable as well as flexible with respect to the physical position of the units. Methods such as master-slave<sup>9</sup>, circular chain control<sup>10</sup> and average load sharing<sup>11</sup> are effective but the major disadvantage of these techniques is that the reliability and flexibility of the system is reduced due to the reliance on crucial intercommunication lines.<sup>12</sup> The crucial high bandwidth intercommunication links between the DGs is absent in the droop method and it uses only local measurement.

One of the main aspects to be considered while designing the control strategy of the microgrid are the output impedances of the parallelly connected inverters. The inverters can possess various types of output impedances such as resistive (R-inverters), inductive (L-inverters), capacitive (C-inverters), resistive-inductive ( $R_L$ -inverters) or resistive-capacitive ( $R_C$ -inverters). In majority of the cases the output impedances of the inverters are inductive

owing to the presence of the line impedance and the filter but in the case low power systems, the inverter has an output impedance that is predominantly resistive. The output impedance of an inverter can easily be changed to be inductive, capacitive, resistive, or complex using various control strategies depending upon the requirement. The inverters with resistive output impedance are believed to be superior to the inverters with inductive output impedance due to the easier compensation of harmonics. In situations where the influence of nonlinear loads on the THD of the voltage needs to be compensated more effortlessly, it is more beneficial to modify the output impedance of the inverter to be resistive since the impedance does not vary with frequency. Recent studies have shown that inverters with capacitive output impedance provide the lowest Total Harmonic Distortion along with superior regulation of voltage while also maintaining accurate sharing of the active and reactive power. On the whole, inverters with capacitive output impedance improves power quality and inverters resistive output impedance enhances system damping when compared to inverters with inductive output impedance.

It is eminent that the droop equations vary for inverters with various types of output impedances.<sup>13</sup> In this paper, the various droop controller strategies for inverters with resistive, inductive, and capacitive output impedances are reviewed. The droop controller equations for the above-mentioned inverters are derived in section II. An overview on how to modify the output impedance of an inverter to be capacitive in order to benefit from the various advantages it offers with respect to the performance of the system is also presented here along with an overview of droop control strategies for inverters with resistive and inductive output impedances. The universal droop controller utilized for controlling inverters in a microgrid irrespective of the kind of output impedance is also presented here. The case studies along with the standards and policies related to microgrids are provided in section III along with the challenges in microgrid implementation. The conclusion is given in section IV.

## 2 Materials and Methods

### 2.1 Droop equations for inverters with various kinds of output impedance

One of the most commonly used control strategies for parallelly operated inverters is the droop control

where the main advantage lies in the absence of the external communication mechanism. The droop approach differs depending on the output impedance of the inverters<sup>14,15</sup> and varies for inverters with various kinds of output impedances. The output impedance of an inverter performs a crucial role in the sharing of power and the inverters can be devised to exhibit various kinds of output impedances depending on the performance aspects that are desired by the system. When the inverter is represented by means of a voltage source in series with an output impedance of  $Z_0$ , the active and reactive power equations are derived as given below in Eqs (1)-(2),

$$P = \left( \frac{EV_0}{Z_0} \cos \delta - \frac{V_0^2}{Z_0} \right) \cos \theta + \frac{EV_0}{Z_0} \sin \delta \sin \theta \quad \dots (1)$$

$$Q = \left( \frac{EV_0}{Z_0} \cos \delta - \frac{V_0^2}{Z_0} \right) \sin \theta - \frac{EV_0}{Z_0} \sin \delta \cos \theta \quad \dots (2)$$

where,  $\delta$  is the power angle which is the phase difference amid the source and the load. The droop equations for inverters with various kinds of output impedances are explored below.

For an inverter with an inductive output impedance, the impedance angle  $\theta$  is  $90^\circ$ . Therefore, the modified real and reactive power equations are given below in Eq. (3),

$$P = \frac{EV_0}{Z_0} \sin \delta \quad \text{and} \quad Q = \frac{EV_0}{Z_0} \cos \delta - \frac{V_0^2}{Z_0} \quad \dots (3)$$

when,  $\delta$  is insignificant,  $\sin \delta \approx \delta$  and  $\cos \delta \approx 1$ . Therefore, as given below in Eq. (4),

$$P = \frac{EV_0}{Z_0} \delta \quad \text{and} \quad Q = \frac{E-V_0}{Z_0} V_0 \quad \dots (4)$$

Hence,

$$P \sim \delta \quad \text{and} \quad Q \sim V_0 \quad \dots (5)$$

Hence, the droop equations are of the form as given below in Eq. (6),

$$E = E^* - nQ_L \quad \text{and} \quad \omega = \omega^* - mP_L \quad \dots (6)$$

where,  $\omega^*$  is the rated frequency and  $E^*$  is rated RMS voltage of the inverter.

For an inverter with a resistive output impedance, the impedance angle  $\theta$  is  $0^\circ$ . Therefore, the real and reactive power from Eqs (1)-(2) become,

$$P = \frac{EV_0}{Z_0} \cos \delta - \frac{V_0^2}{Z_0} \quad \text{and} \quad Q = -\frac{EV_0}{Z_0} \sin \delta \quad \dots (7)$$

when,  $\delta$  is insignificant,  $\sin \delta \approx \delta$  and  $\cos \delta \approx 1$ . Therefore, simplifying Eq. (7),

$$P = \frac{E-V_0}{Z_0} V_0 \quad \text{and} \quad Q = -\frac{EV_0}{Z_0} \delta \quad \dots (8)$$

Hence,

$$P \sim V_0 \quad \text{and} \quad Q \sim -\delta \quad \dots (9)$$

Hence, the droop equations are of the form as given below in Eq. (10),

$$E = E^* - nP_R \quad \text{and} \quad \omega = \omega^* + mQ_R \quad \dots (10)$$

where,  $\omega^*$  is the rated frequency and  $E^*$  is rated RMS voltage of the inverter.

For an inverter with a capacitive output impedance, the impedance angle  $\theta$  is  $-90^\circ$ . Therefore, the real and reactive power from Eqs (1)-(2) become,

$$P = -\frac{EV_0}{Z_0} \sin \delta \quad \text{and} \quad Q = -\frac{EV_0}{Z_0} \cos \delta - \frac{V_0^2}{Z_0} \dots \dots (11)$$

when,  $\delta$  is insignificant,  $\sin \delta \approx \delta$  and  $\cos \delta \approx 1$ . Therefore, simplifying Eq. (11),

$$P = -\frac{EV_0}{Z_0} \delta \quad \text{and} \quad Q = -\frac{E-V_0}{Z_0} V_0 \quad \dots (12)$$

Therefore,

$$P \sim -\delta \quad \text{and} \quad Q \sim -V_0 \quad \dots (13)$$

Hence, the droop equations are of the form as given below in Eq. (14),

$$E = E^* + nQ_C \quad \text{and} \quad \omega = \omega^* + mP_C \quad \dots (14)$$

where,  $\omega^*$  is the rated frequency and  $E^*$  is rated RMS voltage of the inverter.

## 2.2 Modifying the output impedance of an inverter such that it is capacitive

As mentioned in the previous sections the output impedance of most of the inverters in a microgrid are inductive in nature whereas the inverters in low voltage microgrids have resistive output impedance which also offers a better performance compared to the former. Although inverters with capacitive output impedances do not occur naturally in microgrids, it is possible to design an inverter with capacitive output impedance. It is shown<sup>16</sup> that the inverters with capacitive output impedance gives the finest performance overall when equated to inverters with inductive and resistive output impedances. The important parameters that were compared were the total harmonic distortion, the power sharing accuracy of the real and reactive power as well as the voltage regulation. It was also observed that the third harmonics in the output voltage of the inverters with capacitive output impedance was rendered almost zero.

The controller which is used to modify the output impedance of the inverter such that it is capacitive is shown in Fig.1 below. The power circuit diagram shown in Fig. 1(a) consists of DC source supplying a single-phase inverter with an LC filter. While designing the controller the H-bridge and the PWM block are ignored as the mean of the control signal  $u_f$  across a switching period is similar to  $u$ . In the one-line diagram shown in Fig. 1(b), the filter is considered to be a part of the load and the reference voltage  $v_r$  is connected to the output voltage  $v_0$  through an output impedance  $Z_0$  with the output current being  $i$ . As noted from Fig. 1(c) it is possible to modify the output impedance of the inverter such that it is capacitive by subtracting the reference voltage  $v_r$  from the inductor current  $i$  passed through an integrator  $1/sC_0$ .

The power circuit diagram consists of DC source supplying a single-phase inverter with an LC filter. While designing the controller the H-bridge and the PWM block are ignored as the mean of the control signal  $u_f$  across a switching period is similar to  $u$ . In the one-line diagram, the filter is considered to be a part of the load and the reference voltage  $v_r$  is connected to the output voltage  $v_0$  through an output impedance  $Z_0$  with the output current being  $i$ . It is possible to modify the output impedance of the inverter such that it is capacitive by subtracting the reference voltage  $v_r$  from the inductor current  $i$  passed through an integrator  $1/sC_0$ .

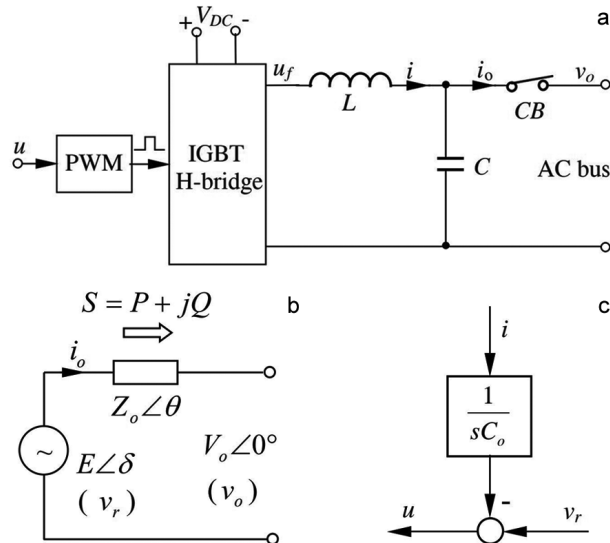


Fig. 1 — Inverter with capacitive output impedance (a) Power circuit diagram (b) Simplified one-line diagram, and (c) Controller for modifying an inverter to have capacitive output impedance.

The equations for the closed-loop system are given below in Eq. (15),

$$u = v_r - \frac{1}{sC_0} i \text{ and } u_f = (R + sL)i + v_0 \quad \dots (15)$$

As the mean of the control signal  $u_f$  across a switching period is similar to  $u$ , Eq. (15) becomes,

$$v_r - \frac{1}{sC_0} i = (R + sL)i + v_0; v_0 = v_r - Z_0(s).i \quad \dots (16)$$

$$\text{where } Z_0(s) = R + sL + \frac{1}{sC_0}$$

A purely capacitive output impedance can be obtained by the inverter at the fundamental frequency if  $C_0$  is insignificant and the influence of the inductor  $(R + sL)$  is not substantial. Therefore, we roughly have,

$$Z_0(s) \approx \frac{1}{sC_0} \quad \dots (17)$$

It<sup>17</sup> has been discovered that the voltage quality is better when the filter inductor is small due to smaller output impedance. According to the current ripple requirements given<sup>18</sup>, the value of the filter inductor  $L$  should satisfy Eq. (18) given below,

$$\frac{5U_{dc}}{8f_s I_{ref}} \leq L \leq \frac{5U_{dc}}{3I_{ref}} \quad \text{where} \quad \frac{U_{dc}}{4Lf_s} = \Delta I \quad \dots (18)$$

At the fundamental frequency, the rated peak current is  $I_{ref}$  and  $\Delta I$  is the inductor current ripple. The filter capacitor is chosen to fulfill Eq. (19) given below,

$$\frac{C_0}{\left(\frac{\pi f_s}{h\omega^*}\right)^2 - 1} \leq C \leq \frac{1}{8} C_0 \quad \dots (19)$$

One of the main factors affecting the total harmonic distortion at harmonic frequencies is the output impedance, which is depicted in Eq. (20) given below,

$$THD = \frac{\sqrt{\sum_{h=2}^{\infty} I_h^2 |Z_0(jh\omega)|^2}}{V_1} \times 100\% \quad \dots (20)$$

Assuming the even harmonics are zero and the odd harmonics are evenly distributed, the optimal value of  $C_0$  can be decided by means of Eq. (21) given below,

$$C_0 = \frac{1}{(\omega^*)^2 L \sum_{h=3,5,7,\dots,N} \frac{1}{h^2}} = \frac{1}{(\omega^*)^2 L \frac{\sum_{h=3,5,7,\dots,N} \frac{1}{h^2}}{(N-1)/2}} = \frac{1}{(\omega^*)^2 L (N-1)/2} \left( \frac{1}{3^2} + \frac{1}{5^2} + \dots + \frac{1}{N^2} \right) \quad \dots (21)$$

where, the number of terms in the computation is  $(N - 1)/2$ .

The optimal value of  $C_0$  while considering a particular  $h$ -th harmonic component is,

$$C_0 = \frac{1}{(h\omega^*)^2 L} \quad \dots (22)$$

Using Eq. (21) certain special cases were solved to figure out the output impedance. For example, in order to minimize the 3<sup>rd</sup> and 5<sup>th</sup> harmonic components the optimal value of  $C_0$  is,

$$C_0 = \frac{17}{225(\omega^*)^2 L} \quad \dots (23)$$

The output impedance is calculated using Eq. (23) as,

$$Z_0(j\omega) = R + j\left(\omega L - \frac{1}{\omega C_0}\right) = R - j\frac{208}{17}\omega^* L \approx -j12.23\omega^* L \quad \dots (24)$$

Since  $R$  is usually smaller than  $\omega^* L$ , the output impedance turns out to be capacitive. Exploring another case where the 3<sup>rd</sup> harmonic component alone is minimized yields the similar output. The optimal value of  $C_0$  in this case is given in Eq. (25),

$$C_0 = \frac{1}{(3\omega^*)^2 L} \quad \dots (25)$$

The output impedance here is calculated using Eq. (25) as,

$$Z_0(j\omega) = R + j\left(\omega L - \frac{1}{\omega C_0}\right) = R - j8\omega^* L \approx -j8\omega^* L \quad \dots (26)$$

Hence it is apparent that the output impedance has turned out to be capacitive in this case as well. The last and final case is to minimize the 5<sup>th</sup> harmonic component. The optimal value of  $C_0$  in this case is given below in Eq. (27),

$$C_0 = \frac{1}{(5\omega^*)^2 L} \quad \dots (27)$$

The output impedance here is calculated using Eq. (27) as,

$$Z_0(j\omega) = R + j\left(\omega L - \frac{1}{\omega C_0}\right) = R - j24\omega^* L \approx -j24\omega^* L \quad \dots (28)$$

The output impedance is seen to be capacitive in this case as well.

An application of an inverter with capacitive output impedance is showcased<sup>19</sup> where it is applied in wind farms so as to enhance the overall performance of the power system. The attributes of the droop strategy of inverters with various types of output impedances such as resistive, inductive, and capacitive were studied plus the utilization of the concept of virtual

impedance to acquire a C-inverter for utilization in wind power generation was demonstrated. Models of SVC and STATCOM that are coupled to the wind power system were setup, with improved converters and the validity of these models were verified along with the effect of C-inverters on the system.

### 2.3 Droop control of low voltage microgrids

Microgrids can function at a low-voltage or a medium-voltage distribution level depending on the capacities and the locations of the distributed generators. The low-voltage microgrids are popular since most of the distributed energy sources have comparatively low-power capacities in the range of around a few hundred kilowatts. One unique feature in low voltage microgrids is that the line impedance is predominantly resistive whereas in other cases due to the long distances between the units the line and output impedances are majorly inductive. One major problem with the droop control is that an unbalance in the line impedance or the output impedance causes a degradation in the power sharing. However, the control strategy used determines the output impedance of the inverter, examples of which are given.<sup>20,21</sup> The droop strategy has additional fast control loops to make sure that the output impedance of the inverter is inductive without the use of an additional output inductor. The technique of utilizing the virtual output impedance to modify the output impedance of an inverter to be inductive will be elaborated later on.

The droop strategy of parallel inverters with resistive output impedance is a topic that has not been explored much barring a few examples given.<sup>22,23</sup> However, the droop strategy in parallel connected dc converters has been extensively analyzed<sup>24-30</sup>, where the product of the output current and a constant term is deducted from the reference voltage thereby easily enforcing the resistive output impedance. Applying the resistive droop strategy to parallelly connected inverters offers various advantages like providing automatic harmonic current sharing, providing more damping to the overall system and the sharing of real power is not affected much by the phase errors.

A droop control strategy applied to an inverter with resistive output impedance is used which allows good sharing of active and reactive power along with the sharing of the harmonics prevalent in the load is given.<sup>31</sup> Here the virtual impedance loop is utilized to fix the phase as well as the magnitude of the output

impedance of the inverter. The resistive output impedance is realized by drooping the voltage reference proportionally to the current  $i_0$ . Individual values of output impedance are obtained using the higher order current harmonics by subtracting a voltage proportionate to the current harmonic from the reference voltage. The voltage reference is given below in Eq. (29),

$$v_{ref} = v_{ref}^* - R_D i_0 - \sum_{h=3}^{11} (R_h - R_D) i_{oh} \quad \dots (29)$$

where, the resistive coefficient is  $R_h$  and the virtual output impedance is  $R_D$ . The harmonic as well as the fundamental components have separate output impedances due to the above-mentioned loop thereby preventing the THD of the output voltage from increasing excessively.

The regular droop control method is modified<sup>32</sup> so as to enhance the dynamics of the inverters connected parallelly. Assuming that the power angle is small, and the inverters have a resistive output impedance, the P and Q equations calculated using Eq. (1) are given below in Eqs (30 and 31),

$$P = \frac{EV}{R} \cos \phi - \frac{V^2}{R} \approx \frac{V}{R} \cdot (E - V) \quad \dots (30)$$

$$Q = -\frac{EV}{R} \sin \phi \approx -\frac{EV}{R} \cdot \phi \quad \dots (31)$$

From the Eqs (30 and 31) it is evident that P becomes higher with an increase in the output-voltage amplitude, and Q reduces with an increase in the power angle. In the conventional droop strategy, an in-built tradeoff is present amongst the output-voltage regulation and the accuracy in the sharing of active and reactive power and does not consider the above-mentioned behavior. Therefore, the droop equations need boost functions to obtain proper sharing of active and reactive power.

Accordingly, the droop equations for resistive output impedance are modified as,

$$E = E^* - nP - n_d \frac{dP}{dt} \quad \dots (32)$$

$$\omega = \omega^* + mQ + m_d \frac{dQ}{dt} \quad \dots (33)$$

where,  $n$  is the proportional coefficient and  $n_d$  is the derivative coefficient of the real power, and  $m$  is the proportional coefficient and  $m_d$  is the derivative coefficient of the reactive power. Integral terms become unstable and hence are not used in this controller whereas the derivative terms are used to

adjust the transient response avoiding any rise in the highest  $E/\omega$  variations. Stability as well as appropriate transient behavior is ensured by the derivative coefficients whereas the control objectives in the stable state are fixed by the proportional coefficients. The momentary circulating currents among the various segments of the system are minimized by this controller thereby enhancing the dynamic operation of the system as a whole.

Although the droop control of inverters with resistive output impedance offers a few advantages, there are certain drawbacks that need to be considered as well. Since low voltage microgrids have resistive line impedances, there are various problems associated with the droop strategy such as the degradation of accuracy in reactive power control in both stand-alone and grid connected modes in addition to the coupling amongst the active and reactive powers. One method to prevent the coupling of power is the frame rotation of the virtual active and reactive power proposed<sup>33</sup>; but the disadvantage here being the direct sharing of the actual active and reactive power is not possible. Although the power coupling can be averted successfully by using a virtual output impedance, the error in the sharing and control of reactive power is possibly bigger in this method due to the amplified impedance voltage drops. The injection of an additional control signal is recommended<sup>34</sup> in order to enhance the accurate sharing of reactive power although possible line current distortions and increased control complexities are a few disadvantages of this method.

An inductive impedance is presented in a system with resistive impedance<sup>35</sup> due to it being a low voltage network by interfacing the inverter with a virtual inductance that is able to avert the coupling amongst the active and reactive powers and an algorithm for the precise sharing of reactive power and its control has also been proposed.

#### 2.4 Droop control strategies for inverters with inductive output impedance

As mentioned earlier, the output impedance of inverters in most instances are inductive about the fundamental frequency. A lot of study has been done on various droop methods for systems with L-inverters and an outline consisting of the various kinds of droop strategies is given below. Although the conventional droop control method offers various advantages, a compromise amongst the accurate sharing of power plus the deviation in voltage,

excessive reliance on the output impedance of the inverter and unbalanced harmonic current sharing are some of the disadvantages of the conventional droop method. Several methods were proposed to modify the conventional droop strategy in order to overcome the above-mentioned drawbacks. A loop for restoring the frequency was included<sup>36</sup> and an adjustable virtual output impedance was employed.<sup>37</sup> The conventional droop strategy merged together with a derivative block was utilized<sup>38</sup> here. Active and reactive power coupling was avoided with the use of virtual inductance<sup>39</sup> as another method. A loop with a virtual impedance merged with the droop control is propositioned<sup>40</sup> using an SOGI system that improves non-linear load sharing, accomplishes improved THD of the output voltage and is not assusceptible to the noise in the output current. For usage in DC microgrids, a droop strategy with the adaptive control is proposed<sup>41</sup> for the renewable ESSs where in the nth sequence of the state of charge is inversely proportional to the coefficient of the droop strategy. A droop strategy with the adaptive control is proposed<sup>42</sup> for low voltage DC microgrids by utilizing an instantaneous virtual resistance  $R_{droop}$  to eliminate problems such as sharing of load current as well as issues pertaining to the circulating current of dc converters connected in parallel. When single-phase microgrids are operated in stand-alone mode problems such as the sharing of reactive power and THD in the voltage arise and are addressed<sup>43,44</sup> here. A coupling transformer is utilized<sup>45</sup> for high voltage microgrids by recognizing an indication on the high voltage end of the transformer and using it to enhance the sharing of the load as well as the regulation of voltage. An improvement in the accuracy of power sharing along with the reestablishment of the dc bus voltage is achieved in a decentralized scheme is proposed<sup>46</sup> by utilizing an enhanced droop strategy founded on low bandwidth transmission. An improved droop control method<sup>47</sup> is utilized where in the gains in the droop strategy in the P- $\omega$  characteristics are varied dynamically to heighten the dynamic performance of AC microgrid is suggested. The adaptive neuro fuzzy inference system was utilized<sup>48</sup> so as to eliminate the reliance on the parameters of the line along with building a comprehensive droop strategy to regulate both the frequency as well the voltage at the same time in stand-alone microgrids and also to tackle an extensive span of changes in the load. A quadratic droop

strategy<sup>49</sup> for the stabilization of voltage in microgrids is suggested where in the method of circuit theory analysis is applicable since the controller utilized to feedback the voltage is quadratic in the magnitude of the voltage locally. When the microgrid is linked to the main grid and is then switched to the stand-alone operating mode and vice-versa, the transition is smoothed out by altering the voltage-based droop control strategy.<sup>50</sup> Keeping the above-mentioned problems in mind, the traditional droop strategy is altered so as to accomplish seamless transfer between the microgrid operating modes with enhanced dynamic performance.<sup>51</sup> In the islanded mode a derivative controller is merged with the droop control so as to boost the power loop dynamics and when connected to the grid an integral controller is combined with the droop control so that the PCC has precise power factor control. The major categories into which the various droop control strategies fall such as conventional droop control, virtual impedance-based droop control, adaptive droop control, robust droop control and consensus-based droop control are detailed below.

#### 2.4.1 Conventional droop control method

The traditional droop strategy is the P-f and Q-v strategy where a decrease in the real power input reduces the frequency, and the voltage relatively increases with the increase in reactive power output to the load. Equations for the traditional droop strategy along with the graphs have been explained in previous sections and will not be gone into detail here. The control diagram for the traditional droop strategy is given below in Fig. 2.

Here  $E^*$  is the voltage reference and  $\omega^*$  is the frequency reference whereas  $n_i$  and  $m_i$  are the droop coefficients. The major benefit of the conventional droop strategy is the absence of significant communication linkages, high flexibility as well as great dependability. However, poor voltage regulation, disparity in line impedance, sluggish response in the transient state, inferior working with distributed generation along with ineffective sharing of the harmonic load are some of the drawbacks.<sup>52-56</sup>

#### 2.4.2 Droop technique using virtual impedance

A virtual impedance<sup>57</sup> may be utilized to improve the efficiency of the P-Q droop strategy. The above-mentioned technique makes the line to which the inverter is connected inductive and is applied at the

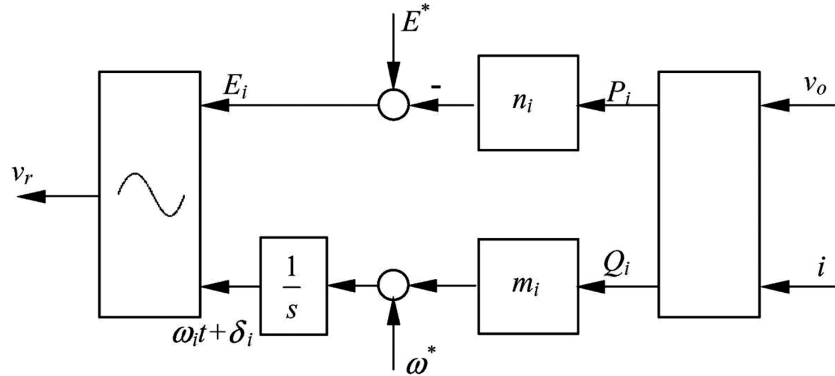


Fig. 2 — Control diagram of the traditional droop strategy.

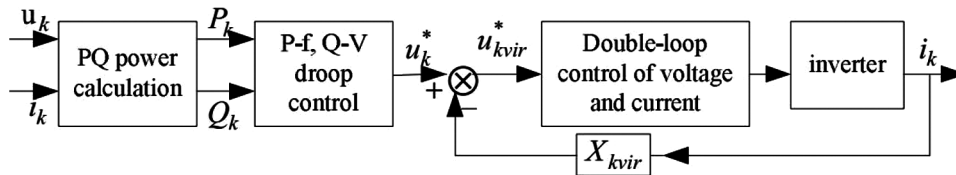


Fig. 3 — Droop technique using Virtual Impedance.

output side. Balanced sharing of reactive power was achieved in several studies as a result of implementing the droop control based on virtual impedance as a quick loop that imitates impedance of the line.<sup>58,59</sup> The control scheme of the droop technique using virtual impedance is given below in Fig. 3.

Here  $u_k^*$  is the voltage reference and k quantity of parallelly connected DGs for a structure inclusive of the virtual impedance. The voltage of the virtual impedance  $X_{kvir}$  is subtracted from the voltage reference  $u_k^*$ . Here it is presumed that the virtual inductance  $L_{kvir}$  dominates while the virtual resistance remains very small.<sup>60</sup> Therefore, with the virtual impedance included, a new voltage reference  $u_{kvir}^*$  is generated for the inverter interfaced with the DGs thereby obtaining an equivalent impedance which is inductive. The major advantages of this method are better voltage harmonic sharing, accurate sharing of reactive power and stable operation whereas the sharing of active power is quite poor.<sup>61-64</sup>

**2.4.3 Adaptive droop control method**

The adaptive droop strategy was suggested in 2002 to provide accurate reactive power sharing while maintaining considerable voltage magnitude.<sup>65</sup> The adaptive droop control method uses the following algorithm: If  $Q_{max} < Q_{ref}$ , the amplitude of the voltage adheres to the conventional reactive power/voltage droop equation<sup>66</sup>, else the voltage

amplitude will be calculated as given below in Eq. (34),

$$E = E^* - nQ - n_{add}(Q - Q_{ref}) \quad \dots (34)$$

where,  $Q_{max}$  is the highest reactive power that can be obtained from every unit and  $Q_{ref}$  is the reactive power reference. Figure 4 given below shows the primitive idea of the adaptive droop strategy.

When  $Q > Q_{ref}$ , the amplitude of the voltage shifts from line 10 to 11 and from line 20 to 21. When  $Q < Q_{ref}$  it can be noticed that the amplitude of the voltage returns to line 12 from line 11 and to line 22 from line 21 instead of getting back to lines 10 and 20 respectively since the maximum reactive power is stored and  $n_{add}(Q - Q_{ref})$  is deducted from the magnitude of voltage. This phenomenon can be expressed using Eq. (35) given below:

$$E = E^* - nQ - n_{add}(Q_{max} - Q_{ref}) \quad \dots (35)$$

The adaptive droop strategy responds well to transients and appropriately shares power, but the circulating current has to be curtailed by using a virtual reactance.<sup>67-71</sup>

**2.4.4 Robust droop control method**

A key drawback of the conventional droop strategy is the error in the sharing of the load proportionally.



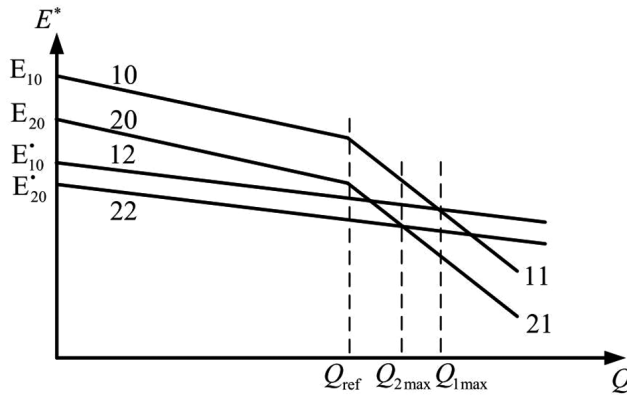


Fig. 4 — Primitive idea of the adaptive droop strategy.

The major reason for this drawback is that the required conditions such as generating similar target values for the inverter voltages as well as parallel inverters having similar per-unit impedances are practically challenging to meet. The robust droop controller was introduced to overcome these drawbacks as well as to reduce the drop in voltage owing to the droop and load effect. The block diagram in addition to the equations of the robust droop technique are similar to that of the universal droop technique given in the later sections. The input to the integrator ought to be zero during the steady state therefore,

$$K_e(E^* - V_0) = nP \quad \dots (36)$$

Given that  $K_e$  is selected to be similar, all the parallelly connected inverters have the same  $K_e(E^* - V_0)$ . Hence Eq. (37) becomes,

$$n_i P_i = constant \quad \dots (37)$$

Although the value of  $E_i$  is not the same, the precise sharing of active power is assured due to this. Neither the output impedance of the inverter nor the disruptions and mathematical mistakes affect the accurate sharing of the active power. It is also well known that for R-inverters as in this instance, the accurate sharing of reactive power is guaranteed since the frequency at which inverters function when the system is stable is similar. A few other advantages of the robust droop controller are that it ensures stability along with the effective regulation of the frequency as well as the voltage. However, the high THD of the current components is the major disadvantage here.<sup>72-74</sup>

#### 2.4.5 Consensus based droop control method

An improved technique of the conventional droop method established on the consensus and sparse

communication network was presented.<sup>75</sup> Two new terms namely  $p_i$  and  $q_i$  are added to the restoration mechanism as an identical R/X ratio leads to losses in the microgrid.  $L_{ij}$  is another term that has been included and  $L_{com}$  which is the last term is the matrix of communication between the DG interfaced inverters. The closed loop dynamic of the proposed method ensures stability, and this is illustrated by establishing expressions along with the simulation of an example consisting of a microgrid with four nodes and three inverters. The biggest advantage of this method over the non-consensus method is the accuracy of the sharing of reactive power among the DG interfaced inverters.

#### 2.5 Universal droop controller

From the previous sections it can be seen that inverters with various kinds of output impedances exist or can be created in order to utilize the benefits that each of these distinct varieties of output impedances offer. Moreover, it has been shown that the droop equations for each of the three kinds of output impedance varies and are unlike the other two cases. For example, in the case of inverters with inductive output impedance, the active power is related to the frequency and the reactive power is related to the output voltage amplitude. However, in the case of inverters with resistive output impedance, the active power is associated with the amplitude and the reactive power is associated with the output voltage frequency. Hence the droop equations have to be changed for every inverter with a different output impedance whose angle also is required to be recognized beforehand so as to implement the droop strategy with the right equations. To surmount this drawback a universal droop strategy was propositioned for inverters with distinct kinds of output impedances.<sup>76</sup>

Prior to the existence of the universal droop control of inverters it was not possible to control inverters with various kinds of output impedances in a parallel manner. The robust droop technique<sup>77</sup> is recommended for inverters with resistive output impedance and is utilized to implement the universal droop strategy which in turn is capable of being implemented on all inverters with no prior knowledge about their impedance angles. The universal droop strategy has been shown to remain stable through impedance angles ranging from  $-90^\circ$  to  $90^\circ$  via small signal stability analysis when applied to an inverter.

The droop controller equations along with the input/output droop relationships for inverters with various kinds of output impedance such as inductive, capacitive, resistive, resistive-capacitive, resistive-inductive are summarized in Table 1 below.

The analysis of parallelly connected of inverters with various kinds of output impedances is done using the orthogonal transformation matrix. Some work has been done previously on the operation of parallelly connected inverters with various kinds of output impedances while restricted to certain types.<sup>78-80</sup> For example, in order to study the working of parallelly connected L, R and R<sub>L</sub> inverters, the following procedure is followed. The orthogonal transformation matrix is given below in Eq. (38),

$$T_L = \begin{bmatrix} \sin \theta & -\cos \theta \\ \cos \theta & \sin \theta \end{bmatrix} \quad \dots (38)$$

When  $\theta$  ranges from 0 to  $\pi/2$  radians the active and reactive power are converted using Eq. (39) into,

$$\begin{bmatrix} P_L \\ Q_L \end{bmatrix} = T_L \begin{bmatrix} P \\ Q \end{bmatrix} = \begin{bmatrix} \frac{EV_0}{Z_0} \sin \delta \\ \frac{EV_0}{Z_0} \cos \delta - \frac{V_0^2}{Z_0} \end{bmatrix} \quad \dots (39)$$

If  $\delta$  is presumed to be minor, from Eq. (39),  $P_L \sim \delta$  and  $Q_L \sim E$  and the droop equations obtained are,

$$E = E^* - nQ_L \quad \text{and} \quad \omega = \omega^* - mP_L \quad \dots (40)$$

It can be seen from Eq. (37) that the droop equations for this converter called the R<sub>L</sub> converter are similar to that of the L inverter. When a similar operation is performed on the parallel operation of R<sub>C</sub>, R and C inverters it can be seen that the droop equations obtained for the R<sub>C</sub> converter are similar to that of C inverters ( $P_C \sim -\delta$  and  $Q_C \sim -E$ ). In order to draw this conclusion prior knowledge of the angle of impedance is necessary in both the cases. On

Table 1 — Input-Output relationships for inverters with various kinds of output impedances

Inverter Type	$\theta$	Input-Output /Droop relationship	Droop Controller
L –	$\frac{\pi}{2}$	$P \sim \delta$ $Q \sim E$	$E = E^* - nQ$ $\omega = \omega^* - mP$
R –	$0^\circ$	$P \sim E$ $Q \sim -\delta$	$E = E^* - nP$ $\omega = \omega^* + mQ$
C –	$-\frac{\pi}{2}$	$P \sim -\delta$ $Q \sim -E$	$E = E^* + nQ$ $\omega = \omega^* + mP$
R <sub>C</sub> –	$(-\frac{\pi}{2}, 0)$	Coupled	Depends on $\theta$
R <sub>L</sub> –	$(0, \frac{\pi}{2})$	Coupled	Depends on $\theta$

further developing the R<sub>L</sub> and R<sub>C</sub> converters it has been shown that it is possible to employ the R<sub>L</sub> controller to inverters with the impedance angles ranging from 0 to 90degrees ( $P \sim P_L \sim \delta$  and  $Q \sim Q_L \sim E$ ) and the R<sub>C</sub> controller to inverters with impedance angles ranging from -90 to 0 degrees ( $P \sim P_C \sim -\delta$  and  $Q \sim Q_C \sim -E$ ).

Similar to the above analysis the transformation matrix given below in Eq. (41) is used to transform the real and reactive power into the following,

$$T = \begin{bmatrix} \cos \theta & \sin \theta \\ -\sin \theta & \cos \theta \end{bmatrix} \quad \dots (41)$$

$$\begin{bmatrix} P_R \\ Q_L \end{bmatrix} = T \begin{bmatrix} P \\ Q \end{bmatrix} = \begin{bmatrix} \frac{EV_0}{Z_0} \cos \delta - \frac{V_0^2}{Z_0} \\ \frac{EV_0}{Z_0} \sin \delta \end{bmatrix} \quad \dots (42)$$

Eq. (42) can be rewritten as follows,

$$P_R + jQ_R = P \cos \theta + Q \sin \theta + j(-P \sin \theta + Q \cos \theta) = e^{-j\theta}(P + jQ) \quad \dots (43)$$

Figure 5 given below shows how the transformation matrix spins the power vector which is P+jQ in the clockwise direction by  $-\theta$  on top of the horizontal line associated with the R inverter for impedance angles that range from 0 to  $\pi/2$  radians and counter-clockwise for impedance angles that range from  $-\pi/2$  to 0 radians.

The eigenvalues of the transformation matrix are  $\cos \theta \pm j \sin \theta$  and it can be seen that the real part being the cosine term is positive for all the angles of impedance ranging from -90 to 90 radians. The real and reactive power are found to have positive associations with P<sub>R</sub> and Q<sub>R</sub> respectively, according to the mapping done using the transformation matrix as well as the linear transformation properties mentioned here.<sup>81</sup> The portrayal of this is given below in Eq. (44),

$$P \sim P_R \quad \text{and} \quad Q \sim Q_R \quad \dots (44)$$

For a small  $\delta$ , the mapping equation gives,

$$P_R \sim E \quad \text{and} \quad Q_R \sim -\delta \quad \dots (45)$$

Combining Eqs (44)-(45) gives,

$$P \sim P_R \sim E \quad \text{and} \quad Q \sim Q_R \sim -\delta \quad \dots (46)$$

For all the angles of impedance ranging from -90 to 90degrees.

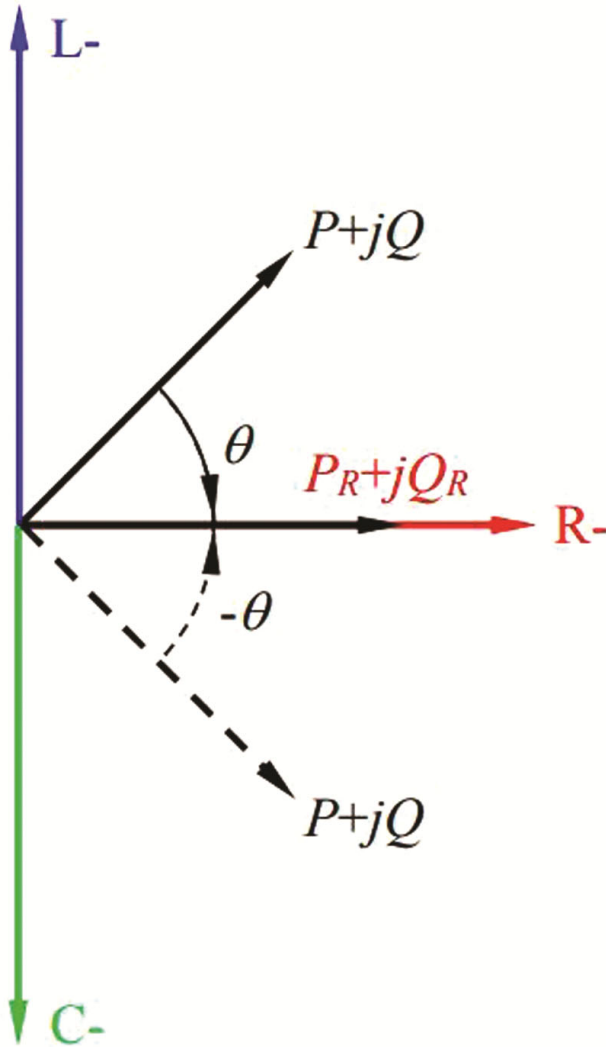


Fig. 5 — Interpretation of the transformation matrix T.

Therefore, from the above analysis the droop equations for the universal droop controller are given below in Eq. (47),

$$E = E^* - nP \quad \text{and} \quad \omega = \omega^* + mQ \quad \dots (47)$$

It can be seen that for all the angles of impedance ranging from -90 to 90 degrees, the active power consistently has a positive relationship with voltage and the reactive power has a negative relationship with frequency which is similar to the droop equation for inverters with resistive output impedance. Theoretically this relationship does not hold when the angle of impedance is completely capacitive ( $\theta = -90$  degrees) or completely inductive ( $\theta = 90$ degrees), but practically, an equivalent series inductor (ESR) is always present along with the inductor used as the filter. Therefore, this strategy is valid for all pragmatic L, C, R,  $R_L$  and  $R_C$  inverters.

The block diagram of the universal droop strategy is given below in Fig. 6, and as seen it utilizes the conuration of the robust droop strategy as mentioned earlier. Hence the advantages of the robust droop control method are carried forward here as well.

The equations of the universal droop controller are described below using Eq. (48),

$$\dot{E} = K_e(E^* - V_0) - nP \quad \text{and} \quad \omega = \omega^* + mQ \quad \dots (48)$$

In the steady state Eq. (48) becomes,

$$nP = K_e(E^* - V_0) \quad \dots (49)$$

Thereby the equation of the output voltage from Eq. (49) becomes,

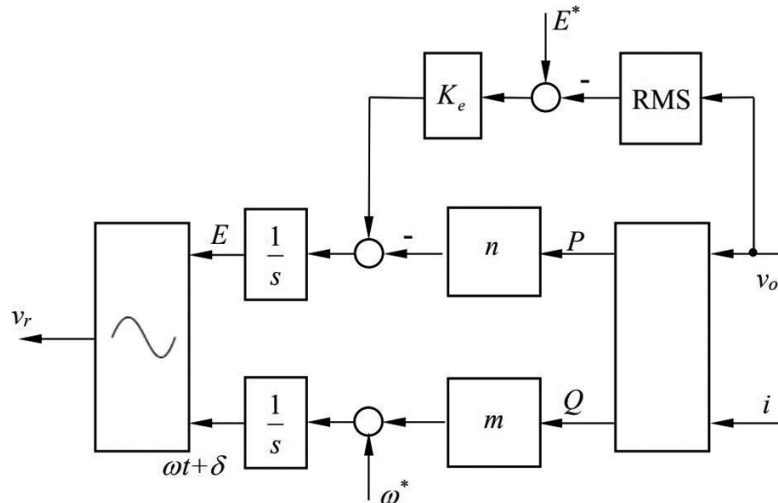


Fig. 6 — Universal Droop Controller Implementation.

$$V_0 = E^* - \frac{nP}{K_e E^*} E^* \quad \dots (50)$$

Therefore, it is apparent that accurate sharing of active power is guaranteed as long similar values of  $K_e$  are chosen for each of the parallelly operated inverters, making one side of the equation similar.

The design and feasibility of the universal droop controller was verified<sup>82</sup> by connecting inverters of different output impedances in parallel and analyzing the performance of the system. Two inverters with capacities 0.5 KVA and 1 KVA were connected in parallel and various possible combinations of output impedances were applied namely L&R, L&L, C&C<sub>R</sub>, C&C, R&R, C<sub>R</sub>&C<sub>R</sub>, L&C, L&C<sub>R</sub>, R&C, R&C<sub>R</sub>, etc. According to the capacities of the inverters it is predictable that  $P_2=2P_1$  and  $Q_2=2Q_1$ . It has been shown that the droop strategy functioned in a satisfactory manner for each of the above-mentioned cases without causing any volatility in the system. In addition to that, proper regulation of voltage and frequency has been sustained in the system irrespective of the type of output impedance present in the inverters. The expected accuracy in the sharing of real as well as reactive power was achieved with a ratio of 2:1. The dynamic performance was also seen to be fast enough with very little overshoot.

### 3 Results and Discussion

#### 3.1 Microgrid implementation in real world scenarios

A case study was done in Peru in February 2021 where in a hybrid Wind and PV microgrid along with a battery storage was utilized for the electrification of rural areas.<sup>83</sup> There are roughly around 1.5 million people in Peru who do not have access to electricity and this microgrid was set up in Laguna Grande, Ica where a rural fishing village comprising of 35 families have been living there for the past 40 years with no access to electricity. This location has a mean irradiation of 6 kWh/m<sup>2</sup>/day annually and an enormous potential of wind energy close to around 8 m/s therefore the microgrid installed here comprises of two wind turbines having a capacity of 3 kW each and a 6 kW<sub>p</sub> photovoltaic system. All the loads in the community are connected to the 230 V AC distribution line and two coupled 4 kW inverters supply power to this line. A 48 V, 800 Ah VRLA (Value Regulated Lead-Acid) battery, designed to function at 50% DOD (Depth of Discharge) is utilized to store energy. A nearly stable power of 1 to 1.2 kW has been contributing to the average day-to-day

demand of 23 kWh proving the effectiveness of the installed microgrid. Technical issues, intermittent nature of the sources and peak surges in demand have contributed to the 10% loss of load during the 2 years of monitoring. Nearly around 60% of the demand is for the nights and hence PV/wind integration is very important. The LCOE (Levelized Cost of Electricity) obtained by the project was 0.267 USD per kWh with its CAPEX reaching 36,000.00USD. The electronics in this project have to be renewed every 10 years and the battery every 3 years with the useful life of this project being about to 20 years.

Another case study was done by ABB Pte. Ltd., Singapore in 2019 for Industry Co, a glass factory situated in India experiencing regular outages.<sup>84</sup> Due to an unreliable grid, this factory faced production losses, lowered workforce efficiency as well as machine/equipment damage. Although the plant utilizes a diesel generator most of the time to reduce the effect of outages, problems like gradual start up times (close to 15 seconds), excessive maintenance and fuel costs and harmful environmental impacts leading to operational intermissions of delicate production equipment persist. Uninterrupted power supplies seem to bridge this gap but come with a substantial cost including maintenance, replacement, and capital costs along with consuming lots of energy and has an efficiency of 96% or less. Microgrids seems to be a good alternative to this issue and are competent of decreasing the drive down costs on the whole as well as the carbon emissions.<sup>85-90</sup> Therefore, a microgrid was utilized only for critical loads that will cause production stoppage even for small power outages. Considering the base case as grid + diesel, three implementation scenarios such as grid + diesel + BESS (Battery Energy Storage Station), grid + diesel + solar PV and grid + diesel + BESS + solar PV were optimized by utilizing the HOMER Pro microgrid modelling software. It was found that the highest IRR (Internal Rate of Return) of 35% was possible with the grid + diesel + BESS scenario which aids in decreasing the costs associated with outages. Nevertheless, the most optimum solution was found to be the diesel + grid + solar PV + BESS scenario where in a maximum of 45% decrease in fuel costs were achieved, along with a 19% reduction in LCOE and a 26% IRR. Along with this the BESS also provides additional benefits such as postponed cost of extra DGs as well as enhanced power quality.

A case study was done in 2018 to assess the feasibility of hybrid microgrids for distant applications in south Cameroon.<sup>91</sup> Nine different cases such as (1) PV + wind + battery, (2) wind + PV + diesel + battery, (3) battery + PV + diesel (4) wind + PV + battery + diesel + small hydro, (5) PV + battery + wind + small hydro (6) battery + PV + small hydro, (7) battery + PV + diesel + small hydro, (8) battery + diesel + wind + small hydro and (9) small hydro + wind + battery were considered. The analysis was done using the HOMER software with the feasibility being depicted primarily based on the CO<sub>2</sub> emissions, NPC, as well as the COE (Cost of Emissions). Among all the above cases, the diesel + PV + battery + small hydrosystem (case 7) gave the most optimal results with a 10-kW diesel genset, a 67.3kW of PV array, 332 units of battery, a 53-kW inverter and a 13.4 kW of small hydro unit. The COE of the above-mentioned system was computed to be 0.443 \$/kWh which is much lower than that of 0.674 \$/kWh that was obtained for case 5 (a pure renewable system). The COE of this system was also found to be lower when compared to two other systems namely a PV + LPG + battery system in North Cameroon and a micro-hydro + LPG + battery system in the South which has COEs of 0.691\$/kWh and 0.355 \$/kWh respectively.<sup>92</sup> This system also generates 170,095 kWh/yr. of power, the composition of which is 57.7% solar, 40.5% small hydro and only 1.84% from the genset. On the basis of its low NPC, COE and system related costs, case 7 seems to be the best economic system in spite of its comparatively high emissions (3.9 x 10.3 kg of CO<sub>2</sub> per year) along with it not being a purely renewable system. Nevertheless, case 5 seems to be the ideal solution from an environmental viewpoint since it has zero emissions and also the second lowest COE. The diesel element in the system is responsible for the carbon dioxide emissions without which the economics of the system decreases (cost increase), favoring its environmental friendliness as well as its sustainability.

### 3.2 Standards and policies related to microgrids

The various obstacles associated with technology, business and policy make it difficult to adopt microgrids in the existing power system. Nevertheless, the elimination of these barriers will significantly enhance the incorporation and installation of microgrids across the world. The policy and regulatory barriers occupy the highest rank amongst all the barriers and there are

numerous standards developing organizations (SDOs) being setup in order to tackle these barriers. The SDOs can be international or regional organizations and are classified according to their field of application, function, and location. SDOs are either profitable or non-profitable organizations and can be funded by either non-government, government, or semi-governmental parties. SDOs regulate the rules along with amending, revising, and coordinating the technical standards for several power system applications. Specifications as well as formal standards are also given by these SDOs, some of which are approved by law and some of which are not but still followed by industries. Some of the highly favored and acknowledged SDOs around the globe are Institute of Electrical and Electronics Engineering (IEEE), International Electrotechnical Commission (IEC), European Committee of Standardization (CEN), International Organization for Standardization (ISO), European Committee for Electrotechnical Standardization (CENELEC), International Telecommunication Union (ITU), Telecommunications Industry Association (TIA), Society of Automotive Engineers (SAE) International, Alliance for telecommunications Industry Solutions (ATIS) and Internet Engineering Task Force (IETF) establishing the norms for smart grid.<sup>93</sup> Standards mainly concentrating on the integration and execution of microgrids has been attended to in the IEEE series and are given below.<sup>94</sup>

The Institute of Electrical and Electronics Engineers (IEEE) Standard 1547 has been a foundational document for the interconnection of distributed energy resources (DER) with the electric power system or the grid. The standards related to microgrids are given in detail in Table 2 below.

The Institute of Electrical and Electronics Engineers (IEEE) 2030 series is a standard for smart grid interoperability of energy and information technologies with the power system. The standard presents an interoperability structure based on cross-cutting technical discipline in information exchange, power application and control through communication. The standards related to microgrids are given in detail in Table 3 below.

In India, the Ministry of New and Renewable Energy (MNRE) has published a draft 'National Policy for Renewable Energy based Micro and Mini Grids' so as to promote the deployment of micro and mini grids driven by renewable energy resources such as wind, solar, hydro, biomass etc.<sup>95</sup> The generating

Table 2 — IEEE 1547 standards related to microgrids

P1547.1 (2005)	The test procedures for the equipment interlinking the Distributed Power System and the electric network are specified.
P1547.2 (2008)	The guideline for the application of IEEE standards during the interconnection is provided.
P1547.3 (2007)	The guideline for monitoring information exchange and control of the Distributed Power System with the power network is drafted.
P1547.4 (2011)	A guideline for operation, integration, and design of Distributed Power System is provided. Moreover, as the draft deals with the operational aspect as well as planning of microgrids, it happens to be a fundamental draft for microgrid operation.
P1547.5 (2011)	The integration of Distributed Power System larger than 10MVA is attended to in this draft.
P1547.6 (2011)	The standards for the interconnection of the Distributed Power System with the secondary network of power system is specified.
P1547.7 (2013)	The important steps of regulating the Distributed Power System and the microgrid is addressed. The methods, and processes to be adhered to are emphasized along with the working steps to examine the influence of the Distributed Power System on the existing power system.
P1547.8 (2014):	The recognition and expansion of the operational procedures, processes, and innovative designs to attain flexibility as well as full utilization of the interconnected Distributed Power System along with the power system is recommended. The industry driven and Smart Grid standards framework are mostly advocated by the P1547.8. Interactive inverters, electric vehicles, multiple Distributed Power System integration, energy storage, interactive utility Distributed Power System operation, voltage-ampere reactive support, multiple Distributed Power System integration, fault ride through, two-way communication are considered by this series of the IEEE 1547 standard.

Table 3 — IEEE 2030 standards related to microgrids

<b>P2030.7 (2017)</b>	Standards for the specification of microgrid are drafted along with the testing procedures. The control methodology for the microgrid energy management system regardless of microgrid's jurisdiction, topology, and configuration are also attended to.
<b>P2030.8 (2018)</b>	The testing standards for microgrid controllers catering to energy management is specified for both islanded as well as grid connected operating modes along with the analysis of the seamless transition amongst these modes of operation.
<b>P2030.9 (2018)</b>	The directions for planning and designing of the microgrids is provided.
<b>P2030.10</b>	The maintenance, design, and operation of DC microgrids for rural as well as urban application is attended to in the draft.

capabilities of the Micro and Mini Grids are designed to be less than 10 kW and more than 10 kW respectively, by means of renewable resources.<sup>96</sup> The

policy proposes to include Energy Service Companies (ESCOs) as Rural Energy Service Providers (RESPs) by offering support along with a few additional privileges so as to increase the number of micro and mini grid projects installed by ESCOs. The RESPs supplying the populations residing in under-served as well as un-served localities like Special Category States (Jammu and Kashmir, Himachal Pradesh, Uttarakhand), Northeast States, Lakshadweep Islands as well as Andaman and Nicobar will be given importance during the distribution of the project. According to the policy, the grids have the flexibility to use either a single source of renewable energy or a hybrid system which utilizes a mixture of renewable energy sources such as solar-biomass, solar-wind, solar-hydro etc. Conventional fuels such as diesel and kerosene cannot be used even for standby functions as per the policy. The additional power produced by the Micro and Mini grids will get transferred to a main grid via interconnections. As per the policy, the specification of the DC microgrid is recommended as 24 V DC up to 1 kWp and 72 V DC from 1 kWp to 10 kWp and that of the AC microgrid as 220 V single phase up to 10 kWp and 440 V three phase beyond that. Financial institutions like NABARD (National Bank for Agriculture and Rural Development), IREDA (Indian Renewable Energy Development Agency Limited), RRBs (Regional Rural Banks) and Commercial Banks are proposed to be included by the policy along with Public Sector Organizations, Village Panchayats and Rural Energy Service Providers while executing the projects.<sup>97</sup> Quick execution of the projects is ensured since the State Nodal (renewable energy developmental) agencies (SNA) are required to grant a straightforward single window clearance.

### 3.3 Challenges in microgrid implementation

Some of the other challenges in the implementation of microgrids are discussed in this section. The weather and the load profile are two big improbabilities that have to be dealt with specially in isolated microgrids since it is not connected to the grid and lacks a bulk power system which can help in maintaining the demand-supply equation. To overcome this challenge energy storage systems like fuel cells, super capacitors and lithium-ion batteries can be utilized to reduce the variability to an extent. Low inertia is another challenge to be considered due to the absence of rotational energy from synchronous machines which cannot be provided by the static

converters that are utilized by renewable energy sources and majority of the Distributed Generators in microgrids are made up of such sources. This leads to critical deviations in frequency in islanded modes if an appropriate control technique is not employed. Synchronverters which are inverters that mimic synchronous generators can be utilized to overcome this challenge by providing frequency control. Another potential solution comes in the form of virtual inertia<sup>98</sup> that can be added into the system in a number of ways in order to dampen the frequency variations in the system. The battery energy storage systems (BESS) can also be controlled to balance the frequency. The transition of the microgrids from grid connected to stand alone modes and vice versa gives rise to stability issues creating transient instability. A lot of research has been done on control techniques that reduce the transient instability and provide a seamless transition between these modes. Synchronization techniques that do not utilize Phase Locked Loops (PLLs) such as self-synchronized synchronverters<sup>99</sup> can also be utilized to provide quick grid synchronization with minimal transients. Modeling a microgrid also seems to be a challenge since most of the characteristics of the traditional systems such as three phase balanced conditions, constant power loads and transmission lines which are primarily inductive are not true for microgrids. There are also several simulation and optimization tools available in the market such as Homer Energy and Distributed Energy Resources Customer Adoption Model (DER-CAM) from Lawrence Berkeley National Laboratory to model the economic and electric effects of microgrids. The Universal droop control technique mentioned in this paper serves as a solution to tackle the problem of variable line output impedances.

#### 4 Conclusion

In this paper the importance of the output impedance of an inverter has been highlighted along with its effect on the control strategy of the microgrid. It has been shown that the output impedance of the parallelly connected inverters changes with the level of voltage in the micro-grid. While in most cases the inverters have inductive output impedance, in the case of low power systems, the inverter has an output impedance that is predominantly resistive. The droop equations for inverters with three varied categories of output impedances have been derived. The technique utilized to achieve a C-inverter has been described and a review of the droop techniques for inverters in

low voltage microgrids which are predominantly resistive have been studied. A summary of the major categories under which the droop techniques aimed at inverters with inductive output impedance fall namely the traditional P-Q droop control method, the droop technique using virtual impedance, the adaptive droop strategy, the robust droop control method, and the consensus-based P-F and Q-V droop control method is given along with a short review. The universal droop strategy which is capable of being utilized for all inverters irrespective of the type of output impedance has been described and an example of a pair of inverters connected parallelly simulated using various combinations of output impedances is also given. The inverters with resistive output impedance are believed to be superior to the inverters with inductive output impedance due to the easier compensation of harmonics. In situations where the influence of nonlinear loads on the THD of the voltage needs to be compensated more effortlessly, it is more beneficial to modify the output impedance of the inverter to be resistive since the impedance does not vary with frequency. From the literature survey it can be concluded that inverters with capacitive output impedance provide the lowest Total Harmonic Distortion along with superior regulation of voltage and frequency while also maintaining accurate sharing of the active and reactive power. On the whole, inverters with capacitive output impedance improves power quality and inverters resistive output impedance enhances system damping when compared to inverters with inductive output impedance. Inverters with capacitive output impedance gives the finest performance overall when equated to inverters with inductive and resistive output impedances. In order to utilize these advantages and improve the overall performance of the system, the output impedance of the inverters can be modified to be capacitive by simply subtracting the reference voltage  $v_r$  from the inductor current  $i$  passed through an integrator  $1/sC_0$ . To the best-known knowledge of the authors, a comprehensive review for droop strategies of inverters with various kinds of output impedances has not been reported in the literature before.

#### References

- 1 Nejabatkhah F, & Li Y W, *IEEE Trans Power Electron.*, 30 (2015) 7072
- 2 [www.dg.history.vt.edu](http://www.dg.history.vt.edu) (20 March 2020)
- 3 [www.smart-energy.com](http://www.smart-energy.com) (22 March 2020)
- 4 [www.marketsandmarkets.com](http://www.marketsandmarkets.com) (22 March 2020)

- 5 www.economictimes.indiatimes.com (22 March 2020)
- 6 www.economictimes.indiatimes.com (23 March 2020)
- 7 www.brookings.edu (23 March 2020)
- 8 www.microgridnews.com (23 March 2020)
- 9 Holtz J, & Werner K H, *IEEE Trans Ind Electron*, 37 (1990) 506
- 10 Wu T F, Chen Y K, & Huang Y H, *IEEE Trans Ind Electron*, 47 (2000) 273
- 11 Sun X, Lee Y S, & Xu D, *IEEE Trans Power Electron*, 18 (2003) 844
- 12 Guerrero J M, Hang L, & Uceda J, *IEEE Trans Ind Appl*, 55 (2008) 2845
- 13 Zhong Q C, & Hornik T, *Control of Power Inverters in Renewable Energy and Smart Grid Integration* (Wiley-IEEE Press, West Sussex), 1st Edn, ISBN: 978-1-118-48179-0, 2013, p. 234
- 14 Brabandere K D, Bolsens B, Den Keybus J V, Woyte A, Driesen J & Belmans R, *IEEE Trans Power Electron*, 22 (2007) 1107
- 15 Guerrero J, Hang L, & Uceda J, *IEEE Trans Ind Electron*, 55 (2008) 2845
- 16 Zhong Q, & Zeng Y, *Can the output impedance of an inverter be designed capacitive* (Proc Int Conf Inf Commun Syst, Melbourne) 2011
- 17 Zhong Q, & Zeng Y, *IEEE Trans Power Electron*, 29 (2014) 5568
- 18 Wu W, He Y, & Blaabjerg F, *IEEE Trans Power Electron*, 27 (2012) 782
- 19 Guo W, & Zhao D M, *Adv Mater*, 10 (2013) 745
- 20 Guerrero J M, De Vicuña L, Castilla M, & Miret J, *IEEE Trans Ind Electron*, 52 (2005) 1126
- 21 Guerrero J M, De Vicuña L, Castilla M, & Miret J, *IEEE Trans Ind Electron*, 53 (2006) 1461
- 22 Wallace K, & Mantov G, *Wireless load sharing of single-phase telecom inverters* (Proc IEEE INTELEC, Copenhagen), 1999
- 23 Chiang S J, Yen C Y, & Chang K T, *IEEE Trans Ind Electron*, 48 (2001) 506
- 24 Jamerson C, Long T, & Mullet C, *Seven ways to parallel a magamp* (Proc IEEE APEC, Los Angeles), 1993
- 25 Johnson B K, Lasseter R H, Alvarado F L, & Adapa R, *IEEE Trans Power Deliv*, 8 (1993) 1926
- 26 Batarseh I, Siri K, & Lee H, *Investigation of the output droop characteristics of parallel-connected dc-dc converters* (Proc IEEE PESC, Taipei), 1994
- 27 Glaser J S, & Witulski A F, *IEEE Trans Power Electron*, 9 (1994) 43
- 28 Perkinson J, *Current sharing of redundant dc-dc converters in high availability systems—A simple approach* (Proc IEEE APEC, Dallas), 1995
- 29 Luo S, Ye Z, Lin R L, & Lee F C, *A classification and evaluation of paralleling methods for power supply modules* (Proc IEEE PESC, Charleston), 1999
- 30 Kim J W, Choi H S, & Cho B H, *IEEE Trans Power Electron*, 7 (2002) 25
- 31 Guerrero J M, Matas J, Vicuna L G, Castilla M, & Miret J, *IEEE Trans Ind Electron*, 54 (2007) 994
- 32 Guerrero J M, Berbel N, Vicuna L G, Matas J, Miret J, & Castilla M, *Droop control method for the parallel operation of online uninterruptible power systems using resistive output impedance* (Proc IEEE APEC, Dallas) 2006
- 33 Brabandere K D, Bolsens B, Keybus J V D, Woyte A, Driesen J, & Belmans R, *IEEE Trans Power Electron*, 22 (2007) 1107
- 34 Tuladhar A, Jin H, Unger T, & Mauch K, *IEEE Trans Ind Appl*, 36 (2000) 131
- 35 Li Y W, & Kao C, *IEEE Trans Power Electron*, 24 (2009) 2977
- 36 Katiraei F, & Iravani M R, *IEEE Trans Power Syst*, 21 (2006) 1821
- 37 Guerrero J M, De Vicuña L, Matas M, Castilla M, & Miret J, *IEEE Trans Ind Electron*, 52 (2005) 1126
- 38 Guerrero J M, De Vicuña L, Castilla M, & Miret J, *IEEE Trans Ind Appl*, 54 (2007) 994
- 39 Li Y W, & Kao C N, *IEEE Trans Power Electron*, 24 (2009) 2977
- 40 Matas J, Castilla M, Vicuna L G, Miret J, & Vasquez J C, *IEEE Trans Power Electron*, 25 (2010) 2993
- 41 Lu X, Sun K, Guerrero J M, Vasquez J C, & Huang L, *IEEE Trans Ind Electron*, 61 (2014) 2804
- 42 Augustine S, Mishra M K, & Lakshminarasamma N, *IEEE Trans Sustain Energy*, 6 (2015) 132
- 43 Micallef A, Apap M, Spiteri-Staines C, Guerrero J M, & Vasquez J C, *IEEE Trans Smart Grid*, 5 (2014) 1149
- 44 Han H, Liu Y, Sun Y, Su M, & Guerrero J M, *IEEE Trans Power Electron*, 30 (2015) 3133
- 45 Shuai Z, Mo S, Wang J, Shen Z J, Tian W, & Feng Y, *J Mod Power Syst Clean Energy*, 4 (2016) 76
- 46 Micallef A, Apap M, Spiteri-Staines C, Guerrero J M, & Vasquez J C, *IEEE Trans on Smart Grid*, 5 (2014) 1149
- 47 Islam S, De S, Anand S, & Sahoo S R, *An Improved Droop Control Method to Enhance Dynamic Performance of AC Microgrid* (Proc NPSC, Tiruchirappalli), 2018
- 48 Bevrani H & Shokoohi S, *IEEE Trans Smart Grid*, 4 (2013) 1505
- 49 Simpson-Porco J W, D'orfler F, & Bullo F, *IEEE Trans in Automat Contr*, 62 (2015) 1239
- 50 Jose J, & Jayanand B, *Simulation and implementation of superlift Luo converter* (Proc ICREESE, Coimbatore), 2013
- 51 Kim J, Guerrero J M, Rodriguez P, Teodorescu R, & Nam K, *IEEE Trans Ind Electron*, 26 (2011) 689
- 52 Tuladhar A, Jin H, Unger T, & Mauch K, *Parallel operation of single-phase inverter modules with no control interconnections* (Proc IEEE-APEC, Atlanta), 1997
- 53 Chandorkar M C, & Divan DM, *Decentralized operation of distributed UPS systems* (Proc PEDES, New Delhi), 1996
- 54 Guerrero JM, Vasquez J C, Matas J, de Vicuna L G, & Castilla M, *IEEE Trans Ind Electron*, 58 (2009) 4305
- 55 Planas E, Gil-de-Muro A, Andreu J, Kortabarri I, & Martínez A I, *Renew Sust Energ Rev*, 17 (2013) 147
- 56 Furtado EC, Aguirre L A, & Torres L A B, *IEEE Trans Circuits Syst II: Express Briefs*, 55 (2008) 1061
- 57 Liu H, Chen Y, Li S, & Hou Y, *Improved droop control of isolated microgrid with virtual impedance* (Proc IEEE PES, Vancouver) 2013
- 58 Skjellnes T, Skjellnes A, Norum L, *Load sharing for parallel inverters without communication* (Proc NORPIE, Stockholm), 2002.
- 59 Zhang G, Jin Z, Li N, Hu X, & Tang X, *A novel control strategy for parallel-connected converters in low voltage microgrid* (Proc IEEE Transp Electr Conf Expo Asia-Pac, Beijing), 2014



- 60 Hidalgo-León R, Sanchez-Zurita C, Jácome-Ruiz P, Wu J, & Muñoz-Jadan Y, *Roles, challenges, and approaches of droop control methods for microgrids*(Proc IEEE PESISGT, Quito), 2017
- 61 Zheng L,Zhuang C, Zhang J, & Du X, *Int J Control Autom Syst*,8 (2015) 63
- 62 Su J, Zheng J, Cui D, li X, Hu Z, & Zhang C, *Engineering*, 5 (2013) 44
- 63 He J, & Li Y W,*IEEE Trans Ind Appl*, 47 (2011)2525
- 64 Wang X, Blaabjerg F, & Chen Z, *An improved design of virtual output impedance loop for droop controlled parallel three-phase voltage source inverters* (Proc IEEE ECCE, Raleigh), 2012
- 65 Kim JW, Choi H S, & Cho B H, *IEEE Trans Power Electron*, 17 (2002) 25
- 66 Tayab U B, Roslan M A B, Hwai L J, & Kashif M,*Renew Sust Energy Rev*, 76(2017)717
- 67 Yang SY, Zhang C W, Zhang X, Cao R X, & Shen W X, *Study on the control strategy for parallel operation of inverters based on adaptive droop method* (Proc ICIEA, Singapore), 2006
- 68 Yao W, Chen M, Gao M, & Qian Z, *Development of communication less hot swap paralleling for single phase UPS Inverters based on adaptive droop method*(Proc IEEE APEC, Washington DC), 2009
- 69 Wei Y, Chen M, Gao M, & Qian Z, *A wireless load sharing controller to improve the performance of parallel-connected inverters*(Proc IEEE APEC, Austin), 2008
- 70 Shafiee Q, Nasirian V, Guerrero J M, Lewis F L, & Davoudi A,*Team-oriented adaptive droop control for autonomous AC microgrids*(Proc IEEE IES, Hangzhou), 2014
- 71 Oureilidis K O, & Demoulias C S, *Sustain Energy, GridsNetw*, 5(2016) 39
- 72 Yao T, Jiang Y, & Ayyanar R,*Single phase DQ frame Glover McFarlane H infinity robust droop controller design*(Proc IEEE IES, Hangzhou), 2014
- 73 Konstantopoulos GC, Zhong Q C, Ren B, & Krstic M,*Bounded droop controller for accurate load sharing among paralleled inverters*(Proc ACC, Portland), 2014
- 74 Konstantopoulos GC, Zhong Q C, Ren B, & Krstic M,*Automatica*,53 (2015) 320
- 75 Lu L, *Consensus-based PF and QV droop control for multiple parallel-connected inverters in lossy networks* (Proc IEEE ISIE, Taipei),2013
- 76 Zhong Q, & Zeng Y, *IEEE Access*, 4 (2016) 702
- 77 Zhong Q, *IEEE Trans Ind Electron*, 60 (2013) 1281
- 78 Brabandere K D, Bolsens B, Den Keybus J V, Woyte A, Driesen J, & Belmans R, *IEEE Trans Power Electron*, 22 (2007) 1107
- 79 Yao W, Chen M, Matas J, Guerrero J M, & Qian Z M, *IEEETrans Ind Electron*, 58 (2011) 576
- 80 Bevrani H, & Shokoohi S, *IEEE Trans Smart Grid*, 4 (2013) 1505
- 81 Poole D, *Linear algebra: A modern introduction* (Brooks/Cole-Cengage Learning, Boston), 2011
- 82 Zhong Q, & Zeng Y, *Parallel operation of inverters with different types of output impedance*(Proc IEEE IECON, Vienna), 2013
- 83 Canziani F, Vargas R, & Gastelo-Roque J A, *Front Energy Res*, 8 (2021) 347
- 84 Mehta R, *A Microgrid Case Study for Ensuring Reliable Power for Commercial and Industrial Sites*(Proc IEEE PES GTD,Bangkok), 2019
- 85 Ipakchi A, & Albuyeh F, *IEEE Power Energy Mag*, 7 (2009) 52
- 86 Son K M, Lee K, Lee D, Nho E, Chun T, & Kim H, *Grid interfacing storage system for implementing microgrid*(Proc IEEE PES T&D, Seoul), 2009
- 87 Bayod-Rújula A, *Energy*, 34 (2009) 377
- 88 Mehta R, Srinivasan D, Khambadkone A M, Yang J, & Trivedi A, *IEEE Trans Smart Grid*, 9 (2018) 299
- 89 Mehta R, Verma P, Srinivasan D, & Yang J, *Appl Energy*, 2 (2019) 146
- 90 Mehta R, Srinivasan D, Trivedi A, & Yang J, *IEEE Trans Smart Grid*, 10 (2019) 523
- 91 Muh E, & Tabet F, *Renew Energy*, 135 (2019) 41
- 92 Nfah E M, Ngundam J M, Vandenberg M, & Schmid J,*Renew Energy*,33 (2008)1064
- 93 Qu M, Marnay C, & Zhou N, *Microgrid Policy Review of Selected Major Countries, Regions, and Organizations* (Lawrence Berkeley National Laboratory, Berkeley), 2011
- 94 IEEE Std 1547-2018, *IEEE Standard for Interconnection and Interoperability of Distributed Energy Resources with Associated Electric Power Systems Interfaces*, (Institute of Electrical and Electronics Engineers, New York), (2018)
- 95 [www.microgridmedia.com](http://www.microgridmedia.com) (April 15, 2020)
- 96 [www.prnewswire.com](http://www.prnewswire.com)(April 15, 2020)
- 97 [www.brookings.edu](http://www.brookings.edu)(April 17, 2020)
- 98 Tamrakar U, Shrestha D, Maharjan M, Bhattarai BP, Hansen TM , & Tonkoski R, *Appl Sci*, 7 (2017) 654
- 99 Zhong Q, Ming W, & Zeng Y, *IEEE Access*, 4 (2016) 7145